Journal of Experimental Marine Biology and Ecology 530–531 (2020) 151429

Contents lists available at ScienceDirect

Journal of Experimental Marine Biology and Ecology

journal homepage: www.elsevier.com/locate/jembe

Parasite development affect dispersal dynamics; infectivity, activity and energetic status in cohorts of salmon louse copepodids

Rasmus Skern-Mauritzen[a,*], Nini H. Sissener[a], Anne D. Sandvik[a], Sonnich Meier[a], Pål N. Sævik[a], Morten D. Skogen[a], Tone Vågseth[b], Sussie Dalvin[a,c], Mette Skern-Mauritzen[a], Samantha Bui[b]

[a] Institute of Marine Research, 5005 Bergen, Norway
[b] Institute of Marine Research, 5984 Matredal, Norway
[c] Department of Biology, University of Bergen, 5020 Bergen, Norway

ARTICLE INFO

Keywords:
Sea lice
Copepod
Lipid metabolism
Pathogen transmission
Dispersal modelling
Ectoparasite

ABSTRACT

The salmon louse, *Lepeophtheirus salmonis,* is a parasitic copepod infecting wild and farmed salmonid fishes in the northern hemisphere. It has a direct lifecycle with a planktonic dispersal phase and an infective copepodid stage preceding five host bound stages. Several models predicting the dispersal of this ecologically and economically important pathogen have been developed, but none include variability in capability to infect. Therefore, the effect of age and temperature on infectivity and lipid metabolism was investigated experimentally using seven synchronized cohorts of copepodids at 5, 10 and 15 °C. In newly molted copepodids infectivity initially increase and then decrease with senescence. Within the experimental temperature range, peak infectivity was higher and occurred earlier at higher temperatures. While degree-days may serve as a useful crude descriptor of developmental age, it did not allow accurate prediction of infectivity peak timing and magnitude unless temperature was included as a separate factor in the derived infectivity model. Senescence was reflected in lipid store depletion and a temperature dependent variability in membrane lipid composition was evident. Interestingly, copepodids developing at 5 °C had approximately 50% less storage lipids when they molted into the parasitic stage than those developing at 10 and 15 °C. The declines in infectivity and storage energy were mirrored in decreasing copepodid swimming activity. When incorporating the copepodid infectivity results from this study into salmon louse dispersal model parameterization, the predictions suggest that earlier models may have underestimated the seasonal differences in salmon louse infection risk.

1. Introduction

Predicting the influence of parasites on their hosts is a key epidemiological challenge that requires accurate knowledge of both pest and host biology (Franceschi et al., 2008; Macnab and Barber, 2012; Mouritsen and Jensen, 1997). Increasing complexity of parasite lifecycle and host-parasite interactions creates more challenges in prediction of epidemiological dynamics. In this landscape, the salmon louse (*Lepeophtheirus salmonis*) emerges as a "species in the middle"; it has a simple transmission requiring no intermediate hosts, but has a relatively complicated lifecycle including stages within both a planktonic and a parasitic niche. While the louse – salmonid host relationship has been the focus of a large number of studies, the planktonic stages have historically attracted less scientific attention (Brooker et al., 2018).

The salmon louse is a copepod ectoparasite of salmonid fishes belonging to the order Caligidae, commonly known as sea lice. It has a lifecycle encompassing eight stages; two planktonic nauplii stages, one infective copepodid stage where the larvae exhibit host-searching behaviours, fueled by a finite energy resource that dictates survival time if a host is not found. If a host is successfully infected, the copepodid stage is followed by two chalimus stages, two mobile preadult stages and lastly, the reproductive adult stage (Hamre et al., 2013). Reproductive females produce eggs organized in eggstrings that remain attached to the female during embryonic development, until hatching as nauplius

Abbreviations: DD, Degree days post hatching (DPH*Temperature in °C); DHA, Docosahexaenoic acid; DPH, Days post hatching; FFA, Free fatty acid; FAME, Fatty acid methyl esters; GC-FID, Gas chromatography - flame ionization detector; GC–MS, Gas chromatography - mass spectrometry; HPTLC, High-performance thin-layer chromatography; MUFA, Monounsaturated fatty acids; PCA, principal component analysis; PL, Polar lipids; PUFA, Polyunsaturated fatty acids; ROC, Relative operating characteristic; TAG, triacylglycerol; TLC, Thin layer chromatography.

* Corresponding author.
E-mail address: rasmus@hi.no (R. Skern-Mauritzen).

https://doi.org/10.1016/j.jembe.2020.151429
Received 1 April 2020; Received in revised form 17 June 2020; Accepted 23 June 2020
Available online 09 July 2020

larvae (Pike and Wadsworth, 1999).

Farming of Atlantic salmon (*Salmo salar*) in the Northern Atlantic has changed the salmon louse host availability drastically: Over a period of a few decades farming has supplied a stable and increasing supply of hosts, in many locations outnumbering wild salmonids by 2–3 orders of magnitude, as illustrated by the Norwegian farmed standing stock of around 400 million Atlantic salmon (www.ssb.no) in contrast to an estimated ≈ 0.5 million wild Atlantic salmon returning to spawn (Anon, 2019). The salmon louse has responded with exploding populations sizes in parallel, and now represent a formidable challenge for marine salmonid aquaculture and wild salmonid populations in the North Atlantic Ocean (Bjørn et al., 2001; Costello, 2009; Finstad and Bjørn, 2011; Fjelldal et al., 2019; Fjørtoft et al., 2019; Forseth et al., 2017; Halttunen et al., 2018; Skern-Mauritzen et al., 2014; Torrissen et al., 2013). Formerly, sea lice infections in farmed salmonids were controlled mainly by administration of antiparasitic pharmaceuticals (Burridge et al., 2010). Since the late 2000's, resistance and decreased sensitivity towards the compounds used have resulted in the emergence of a number of non-chemical delousing strategies including shielding skirts, warm water treatments and use of cleaner fish (Aaen et al., 2015; Gonzalez and de Boer, 2017; Grøntvedt et al., 2015; Oppedal et al., 2017; Stien et al., 2018). Despite the efforts, lice abundances regularly exceed management aims (Myksvoll et al., 2018; Taranger et al., 2015). Lice infection levels are monitored through compulsory routine counts at farms (e.g. Ireland: Montoring Protocol No. 3 for Offshore Finnfish Farms - Sea Lice Montoring and Control. https://www.agriculture.gov.ie, Scotland: The regulation of sea lice in Scotland 2019. Topic Sheet Number 71 (v3). https://www2.gov.scot/, Norway: Forskrift om bekjempelse av lakselus i akvakulturanlegg. 2018. https://lovdata.no/dokument/SF/forskrift/2012-12-05-1140) and through field surveys of wild populations (Myksvoll et al., 2018). Additionally, modelling allows extrapolation of infection risk in areas without observations (Grefsrud et al., 2018; Myksvoll et al., 2018; Sandvik et al., 2020).

Statistical models (Aldrin et al., 2013; Hall and Murray, 2018; Kristoffersen et al., 2014)) and mechanistic models (Adams et al., 2016; Asplin et al., 2014; Johnsen et al., 2014; Salama et al., 2013; Sandvik et al., 2016; Sandvik et al., 2020) have been used to predict salmon lice epidemiology in space and time - and have evolved to reflect observations with a reliability that warrants their use in management decisions (Myksvoll et al., 2018; Nilsen et al., 2017; Sandvik et al., 2016; Sandvik et al., 2020; Skardhamar et al., 2018). Improved parameterization and further development of such models require fundamental understanding of salmon louse dispersal biology and consideration of generalized parasite transmission models (Brooker et al., 2018; McCallum et al., 2017). One of the key traits identified as requiring further information for improved parameterization is the variability in capability of copepodids to infect a host, hereafter referred to as infectivity (Brooker et al., 2018).

Larval development takes approximately 30–50 degree-days from hatching to the infective copepodid and these remain infectious for approximately 90–140 degree-days (Samsing et al., 2016). In present biological-hydrodynamic coupled models, copepodids are considered equally infectious throughout the stage (Myksvoll et al., 2018; Peacock et al., 2020). However, studies on salmon lice infectivity dynamics indicate that copepodids are less infectious immediately after molting and reach peak infectivity after a few days followed by a decrease in infectivity with senescence (Frenzl, 2014; Gravil, 1996; Tucker et al., 2000). Similarly, it has been shown that temperature affects the copepodids' ability to successfully infect a host (Hamre et al., 2013; Samsing et al., 2016). The mechanism underlying the decreasing infectivity in ageing copepodids is widely accepted to be energy depletion. The main energy storage product in salmon lice eggs is triacylglycerol (Lee, 1975; Tocher et al., 2010) and stored energy levels have been shown to gradually decrease in ageing copepodids, although the exact lipid metabolism dynamics remain unknown (Dalvin et al., 2011; Gravil, 1996; Khan et al., 2017; Khan et al., 2018; Thompson et al., 2019; Tucker et al., 2000). However, there is a need for a more detailed study of infectivity profiles allowing their inclusion in dispersal models. In the present study, we firstly describe the temporal infectivity dynamics and behavioral activity across a range of temperatures. Secondly, we describe the temporal changes in the lipidome of the copepodids, with emphasis on understanding the energetic status and lipid composition in ageing individuals. Finally, we explore the impact of our findings on spatiotemporal infection risk by modelling.

2. Materials and methods

2.1. Experimental overview

Cohorts of enumerated *Lepeophtheirus salmonis salmonis* (Skern-Mauritzen et al., 2014) copepodids with defined ages were used to infect four replicate tanks containing ten Atlantic salmon at seven timepoints spanning the copepodid stage. The experiment was performed at 5, 10 and 15 °C. At the time of infection, copepodids were counted, activity levels were assessed, and samples were taken for later lipid analysis. The individual salmon groups were terminated when copepodids had molted to the chalimus I stage (estimated according to (Stien et al., 2005), and the infection levels were determined by counting attached larvae.

2.2. Experimental fish, rearing conditions and husbandry

The experiment comprised of 840 Atlantic salmon (*Salmo salar*), and additional salmon used to maintain a population of salmon lice (see below). The salmon were supplied by AquaGen, originating from their Atlantic QTL-innOva PRIME strain, and were vaccinated with AlphaJect micro 6 on September 12th, 2017 with an average weight of 55 g. Upon completed smoltification, the fish were transferred to seawater on November 2nd.

The experimental fish were introduced in groups of ten to separate 500 l tanks with running sea water at the experimental temperature, at least 5 days prior to infection to allow for acclimatization. Fish were provided a commercial diet using a standard feed regime throughout the experiment. At each experimental temperature, the fish were infected with enumerated cohorts of copepodids at seven defined ages in four replicate tanks; a total of 28 tanks with 280 fish were used at each temperature. The experiment was conducted at 15 °C in November–December 2017, and at 5 °C and 10 °C in February and March 2018. At the experiment conclusion, all fish were euthanized by an overdose of anesthesia (0.1 g/l metomidate hydrochloride, Aquacalm®). In some instances, fish died during the experiment; these were removed from the tanks during the daily inspections and excluded from the dataset. The experiments were conducted at the Matre research station of the Institute of Marine Research, Norway, in accordance with Norwegian legislation for animal welfare, under permit ID 14047 from the Norwegian Food Safety Authority.

2.3. Salmon louse culturing

Adult female salmon lice were collected from farmed fish in Masfjorden on October 6 and 12 2017, and their eggstrings transferred to an incubator with running seawater (Hamre et al., 2009). Once hatched, the resulting copepodids were used to infect 30 adult salmon kept in three 500 l tanks at 10 °C (under permit ID 12935 from the Norwegian Food Safety Authority). Once these lice had developed to adults, the resulting eggstrings were used to produce the experimental copepodid cohorts for the infectivity experiments. Adult female lice produce eggs where embryonic development occur within the eggstring, until nauplius larvae are released during hatching. Almost immediately after hatching, the female extrudes a new pair of eggstrings. For each experimental temperature (5, 10 and 15 °C), the production lice and their hosts were kept at the test temperature for at least one

Table 1
Details of the experimental groups of salmon lice cohorts: across the test temperatures, the ages of copepodid used to infect hosts (days post hatching, DPH), the duration of the time windows used for sampling the cohorts (in days, see section 2.4 main text for further details), infection and termination dates, the numbers of fish infected (#Fish) and fish mortality (#Fish lost), numbers of copepodids used to infect, and the number of replicate tanks.

Temp.	Age (DPH)	Cohort window	Infection date	Termination date	#Fish	#Fish lost	Infection dose	#Replicate tanks
5	10.51	0.29	06.02.2018	20.02.2018	39	0	991	4
5	11.95	0.25	09.02.2018	20.02.2018	67	2	1232	4
5	13.03	0.25	08.02.2018	20.02.2018	35	0	1209	4
5	14.96	0.25	08.02.2018	20.02.2018	37	0	1269	4
5	17.84	0.25	09.02.2018	20.02.2018	40	3	811	4
5	20.93	0.25	13.02.2018	20.02.2018	40	3	1173	4
5	23.34	0.25	16.02.2018	20.02.2018	40	9	742	4
10	4.39	0.26	02.03.2018	08.03.2018	40	0	1217	4
10	5.00	0.21	02.03.2018	08.03.2018	40	0	1247	4
10	6.33	0.33	05.03.2018	08.03.2018	40	0	1223	4
10	7.94	0.16	01.03.2018	08.03.2018	40	0	1190	4
10	11.05	0.21	05.03.2018	12.03.2018	40	1	1232	4
10	14.06	0.16	07.03.2018	12.03.2018	40	1	1223	4
10	16.41	0.27	09.03.2018	16.03.2018	40	0	1477	4
15	2.60	0.07	06.12.2017	15.12.2017	40	0	878	4
15	2.96	0.13	04.12.2017	14.12.2017	40	0	1201	4
15	3.84	0.14	07.12.2017	17.12.2017	40	0	1218	4
15	6.32	0.31	08.12.2017	17.12.2017	40	0	1287	4
15	7.51	0.34	23.11.2017	03.12.2017	40	0	1200	4
15	10.34	0.49	27.11.2017	06.12.2017	40	0	803	4
15	12.67	0.50	28.11.2017	07.12.2017	40	0	664	4

eggstring production cycle to ensure that both vitellogenesis and embryonic development occurred at the experimental temperature.

2.4. Copepodid cohort production and status assessment

As the objective of the experiment was to study the effect of ageing on copepodids, optimal accuracy determination of the time since molting to copepodids was essential. To this end, cohorts of synchronously developing larvae were obtained by incubating a large number of eggstrings, and subsequently harvesting all nauplius larvae that hatched during a defined time window. For logistical reasons, the time window varied from 1 to 12 h and did not exceed 8 h for the four youngest ages at each temperature. Details on cohort production are given in Table 1 and Table S1. The duration of the naupliar stages and resulting age of the copepodids was calculated based on the minimum time from hatching to appearance of copepodids according to Stien et al., (2005).

The larvae were allowed to develop into the predetermined copepodid age in incubators (one incubator cohort^{-1}). At each infection the copepodids were divided into aliquots, rather than individually transferred, to avoid excessive handling. To calculate infection success, the exact densities of lice introduced to experimental tanks were counted before infection (depending on the number of copepodids available doses ranged from 76 to 370 copepodids tank^{-1}, mean = 280, standard deviation = 54, see Table S1). Additionally, prior to infection, a separate subsample of 41–87 copepodids were scored in four activity categories based on Gravil, (1996); 1) totally inactive (i.e. dead or moribund), 2) barely moving upon stimulation (e.g. moving an appendage but apparently unable to swim), 3) active swimming only upon stimulation, or 4) active swimming without stimulation. Larvae were stimulated by expulsion of water from a pipette. Upon stage confirmation and activity determination, the copepodids were placed on a glass-filter in glass vials and frozen at −80 °C for lipid analysis (see section 2.7).

The enumeration and activity assessments were done at 5, 10 and 15 °C and the copepodid cohorts were generated to cover the entire expected survival time for copepodids (estimated from (Samsing et al., 2016)). The cohort ages and additional details at the different temperatures are shown in Table 1 and Table S1.

2.5. Infection procedure

During the infections, water flow was stopped in the tanks and the water level was reduced to 50% before copepodids were introduced into the water (for exact numbers see Table S1). After 20 min, flow was increased to 3 l min^{-1}, and after a further 25 min, normal flow of 10 l min^{-1} was reinstated. Oxygen condition was monitored in the tanks throughout, ensuring that levels higher than 70% were maintained.

2.6. Experiment termination

The experiments were terminated at the time lice were expected to have developed into chalimus I (Table 1 and Table S1), based on the temperature and development rate according to Stien et al., (2005). The fish were euthanized by an overdose anesthetic as described above. All attached salmon lice were counted under a dissecting microscope and the euthanization vessel was scrutinized for detached lice, by staff having passed the research institute's internal salmon louse larvae detection tests (passing requires detection and identification of all stages, including copepodids, present on experimentally infected fish). The observed infectivity (probability of attachment success) was calculated by dividing the total number of lice found on the fish and in the euthanization vessel with the number of copepodids used to infect the tank. Fish that died during the experimental period were routinely removed in collective lots not allowing lice numbers to be reliably enumerated. Thus, in tanks with mortality, the fraction of lice recovered was calculated by excluding a proportion of the copepodids scaled to the proportion of fish lost (i.e. assuming that infection levels on fish were uniform). At 5 °C 17 out of 280 fish died, at 10 °C two out of 280 fish died, while there were no mortality at 15 °C.

2.7. Lipid analysis

Samples of 41–87 copepodids from all temperatures and timepoints were counted and placed on a small piece of glass-filter (Whatman™ 1001–090 Grade 1 Qualitative Filter Paper, Pore Size: 11 μm) and frozen in 1.5 ml glass vials at −80 °C for lipid analysis.

The samples were extracted with 2 × 0.5 ml of chloroform:methanol (2:1). The extract was filtered through a Pasteur pipette with glass wool, to remove tissue residue, in to a 16 ml glass tube.

The extract was evaporated to dryness by N_2 (g) and the lipid was dissolved in 30 µl chloroform:methanol. 15 µl was used for separation of lipid class analysis followed by fatty acid analysis and the remaining 15 µl was used for analysis of total fatty acids in the samples. These were added 10 µg of nonadecanoic acid (19:0) as an internal standard.

Three lipid classes - polar lipid (mixture of phospholipids, PL), neutral lipid (mainly triacylglycerol, TAG) and free fatty acid (FFA) - were separated on high-performance thin-layer chromatography (HPTLC) (10 × 10 cm TLC plates from Merck) according to Olsen and Henderson, (1989). 15 µl of each sample was loaded as a spot to the lower part of the TLC plate using a glass micro-syringe. The TLC plates were developed with a single system (methyl acetate: isopropanol: chloroform: methanol: 0,25% KCl (aq) (25:25:25:10:9 by volume)) until solvent had been absorbed 9 cm up the plate. The three lipid classes were visualized by dichlorofluorescein and UV, carefully scraped off the plate with a razor blade and placed into thick walled glass tubes prepared with 10 µg of internal standard 19:0.

All samples (both the three lipid classes and the unseparated lipid extract) were methylated, and the respective fatty acid methyl esters (FAME) were analysed on a HP-7890A gas chromatograph (Agilent, USA) with a flame ionization detector (GC-FID) according to Meier et al., (2006). As a methylation reagent 2.5 M dry HCl in methanol was used. The FAMEs were extracted using 2 × 2 ml of hexane. Due to the very small samples sizes, the extracted hexane samples were evaporated down to a minimum volume of 50 µl to obtain a suitable chromatographic response. Ten µl were injected splitless (the split was open after 2 min), the injection temperature was set to 280 °C. The column was a 25 m × 0.25 mm fused silica capillary, coated with polyethylene-glycol of 0.25 µm film thickness, CP-Wax 52 CB (Varian-Chrompack, Middelburg, The Netherlands). Helium (99.9999%) was used as mobile phase at 1 ml min^{-1} for 45 min and then increased to 3 ml min^{-1} for 30 min. The temperature of the flame ionization detector was set at 300 °C. The oven temperature was programmed to hold at 90 °C for 2 min, then from 90 °C to 165 °C at 30 °C min^{-1} and then to 240 °C at 2.5 °C min^{-1} and held there for 35 min. Total analysis time was 75 min. 29 peaks in the chromatogram were selected, and identified by comparing retention times with a FAME standard (GLC-463 from Nu-Chek Prep. Elysian, MN, USA) and retention index maps and mass spectral libraries (GC–MS) (http://www.chrombox.org/index.html) performed under the same chromatographic conditions as the GC-FID (Wasta and Mjos, 2013). Chromatographic peak areas were corrected by empirical response factors calculated from the areas of the GLC-463 mixture. The chromatograms were integrated using the EZChrom Elite software (Agilent Technologies).

Possible background contamination: Due to the small size and low fatty acid content (0.14–0.7 µg/individual) of the copepodids, pooled samples of a large number of individuals were used. Even so, the total amount of fatty acids in the extracts ranged from 7 to 37 µg, making the analysis vulnerable for background contamination. Analysis of blank samples that have gone through the whole analytical procedure (Lipid extraction, TLC lipid classes separation, methanolysis and GC-FID analysis) revealed a background of the two saturated FAs; 16:0 and 18:0 in the FFA fraction. To avoid introducing bias in the results, data from the FFA samples were not used in data analysis. Details of the background analysis are given in the supplementary results.

2.8. Statistical analyses

The aim of the study was to improve our understanding of how infectivity and lipid metabolism varies with copepodid age at different temperatures.

To derive an infectivity model, we performed logistic regression on the binary infestation results (successful or unsuccessful infestation judged from counting lice on the fish at experiment termination) from the ageing cohorts of copepodids using age and experimental temperatures as predictors. Developmental age was recorded as days post hatching (DPH) and degree-days post hatching (DD: temperature x DPH). Degree-days is a commonly used parameter in biological-hydrodynamic coupled models and we therefore include DPH and DD when performing the logistic regressions. Since the nauplius II stage preceding the copepodid stage is unable to infect, datapoints with zero infection at the estimated time for molting (Stien et al., 2005) were added to the analysis. Likewise, since dead or moribund copepodids are unable to infect hosts, datapoints with zero infection at 200 DD were added to the analysis. Initial plots suggested curve-linear relationship between infectivity and age that differed depending on temperature. Thus, we fitted polynomial logistic regressions of the form:

$$\text{Log (infection odds)} \sim \alpha + \beta_{T\,Nt}\text{Temp}^{Nt} + \beta_{A\,Na}\text{Age}^{Na} + \beta_{AT\,Na}\text{Age}^{Na} * {}_{Nt}\text{Temp}^{Nt}$$

using a logit link function and assuming a binomial distribution estimating the impact of temperature (βT) and age (βA as DPH or DD) as main effects, as well as interaction effects for the different polynomials of age and temperature (βAT). To identify functions reflecting the general trends in infectivity, we included polynomials of age ($1 \leq Na \leq 4$) and polynomials of temperature ($1 \leq Nt \leq 2$) in the numerical model. Hence, the most complex model included a 4th order polynomial of age, a 2nd order polynomial of temperature and interactions between polynomial age and temperature, treated as a linear, continuous variables. To identify the most appropriate model we included all possible models nested within Eq. (1) in the comparison (selected models shown in Table 2). We ran all the models and selected the best model based on topographic consideration and model comparison using AIC. The chosen model was further assessed using diagnostics including trends in residuals, outliers, dispersion and deviance explained. All statistical analyses were performed in RStudio v. 3.5.3 using the "frm" and "mgcv" packages.

To better understand copepodid lipid metabolism, we performed principal component analysis (PCA) and linear regression on the PL, FFA and TAG lipid composition. The PCAs was carried out in Sirius (version 11.0, PRS, Norway). To make the systematic variation in the PCA independent of variable "size" each variable was weighted divided by its mean before PCA. The linear regressions were performed in XLSTAT, 2019 (Addinsoft, US).

2.9. Modelling infection risk in time and space

We incorporated the age- and temperature-dependent infectivity model derived in section 2.8 into a biophysical salmon lice dispersion model used by the Norwegian national salmon lice monitoring system (Myksvoll et al., 2018; Sandvik et al., 2020). In this model, lice larvae develop as a function of temperature and have a vertical behavior with response to light and salinity. Previously, lice were assigned a fixed infectivity rate inside the range 40 to 170 DD, and zero outside this range. The predictive ability of the old and new formulation was assessed using the relative operating characteristic (ROC) method

Table 2
The most pertinent of the tested models showing the degrees of freedom (DF) for a total of 84 observations, the AIC score and the proportion of deviation explained (DE) by the model. Model terms included temperature (Temp in °C), and larval age as DPH or DD.

Model	DF	AIC	DE
A) DD + DD^2	3	5792	26.3
B) Temp + $Temp^2$ + DD + DD^2 + DD*Temp + DD^2*Temp	7	1913	79.5
C) Temp + $Temp^2$ + Age + Age^2 + Age^3 + Age *Temp + Age^2*Temp + Age^3*Temp	9	1841	80.5
D) Temp + $Temp^2$ + DD + DD^2 + DD^3 + DD^1*Temp + DD^2*Temp + DD^3*Temp	9	1654	83.1
E) Temp + $Temp^2$ + DD + DD^2 + DD^3 + DD^4 + DD^1*Temp + DD^2*Temp + DD^3*Temp + DD^4*Temp	11	1258	88.6

described in Sandvik et al. (Sandvik et al., 2016; Sandvik et al., 2020). The ROC is a graph of the hit rate, H, against the false alarm rate, F, for different decision thresholds (Mason, 1982), developed based on observations from sentinel cages in the Hardangerfjord for the years 2012–2017. The sentinel cage data and ROC-output uses three categorical events (high, medium, and low) for the lice infestation pressure, and is at present in use as components of the "Traffic-light system" for a sustainable management of Norwegian salmon farming (Vollset et al., 2019). Forcing for the dispersion model (currents, temperature and salinity) was provided by a hydrodynamic fjord model with horizontal resolution of 160 m × 160 m, and 35 vertical sigma layers (Albretsen et al., 2011; Skardhamar et al., 2018).

In addition to the ROC evaluation based on realistic parameterization, we also performed idealized simulation model experiments to visualize the impact of temperature on the infection risk. In our model experiment, 5 virtual sea lice particles (each representing 100,000 eggs) were released per hour from a source in the Hardangerfjord over the period March 2 to August 15, 2019. We then computed the mean infecion pressure on a regular 500 m × 500 m grid, under three constant water temperature scenarios (5, 10 and 15 °C), for both the old and new infectivity model. Infection risk was defined as the infectivity-scaled particle density. To make the results comparable, the new infectivity formulation was scaled by parameters obtained from the ROC assessment.

3. Results

3.1. Copepodid activity and infectivity

The results showed that infectivity initially increased after molting into copepodids and subsequently declined with senescence, at all investigated temperatures (Fig. 1A). The observed infectivity was positively correlated with temperature and the peak values observed were 65% at 3 DPH and 15 °C, 43% at 11 DPH and 10 °C, and 24% at 21 DPH and 5 °C. Peak infectivity were several times greater than infectivity observed for preceding or succeeding ages. Furthermore, the peaks occurred in younger age cohorts at higher temperatures than at colder temperatures. Activity of the copepodids declined with time and thus mirrored the infectivity and storage lipid declines (see below). Interestingly, activity appeared stable until a point where after it dropped abruptly at a time coinciding with declining infectivity (Fig. 1B and C). Furthermore, there was no initial increase in activity that mirrored the initial increase in infectivity (Fig. 1B).

3.2. Infectivity model

Several statistical models including those shown in Table 2 were evaluated. Including polynomial temperature and age (as DPH or DD) as predictors increased the explanatory power and improved the model fit relative to simpler models. Models including age as a 4th-order polynomial had higher explanatory power and better AIC scores than the simpler models. However, examination revealed that such models were overfitted and exhibited unrealistic topologies (e.g. > 1 infestation peak) compared to lower order models.

Both models C and D reflected the data quite accurately, and ultimately model D (Fig. 1C) was selected based on its lower AIC score, higher explanatory power and easier implementation in biological-hydrodynamical coupled models. An ANOVA test on model parameters demonstrated that all terms were highly statistically significant ($p < 10^{-10}$). Retrieving parameters from model D yielded Eq. (1). for estimating log infectivity (Ln(I)) under the present experimental conditions.

$$\mathrm{Ln(I)} \sim -34.660 + 2.306\,T - 2.585e-2\,T^2 + 7.156e-1\,A - 5.354e-3\,A^2 + 1.191e-5\,A^3 - 3.577e-2\,AT + 2.526e-4\,A^2T - 5.541e-7\,A^3T \quad (1)$$

Where T is temperature in °C and A is age as DD. The infectivity (probability of attachment success, I) can be calculated from:

$$I = e^{\ln(I)}/(1 + e^{\ln(I)}) \quad (2)$$

If the age is desired as time since hatching into copepodids, the age will have to be offset by the developmental time for the nauplius stages which can be estimated according to Stien et al. (Stien et al., 2005):

$$\text{Development time (days)} = \tau(T) = (\beta 1/(T - 10 + \beta 1\,\beta 2))^2 \quad (3)$$

Where T is temperature in °C, $\beta 1 = 24.79$ and $\beta 2 = 0.525$.

3.3. Energy depletion and lipid metabolism

Total lipid content was reduced over time in all groups, driven by a

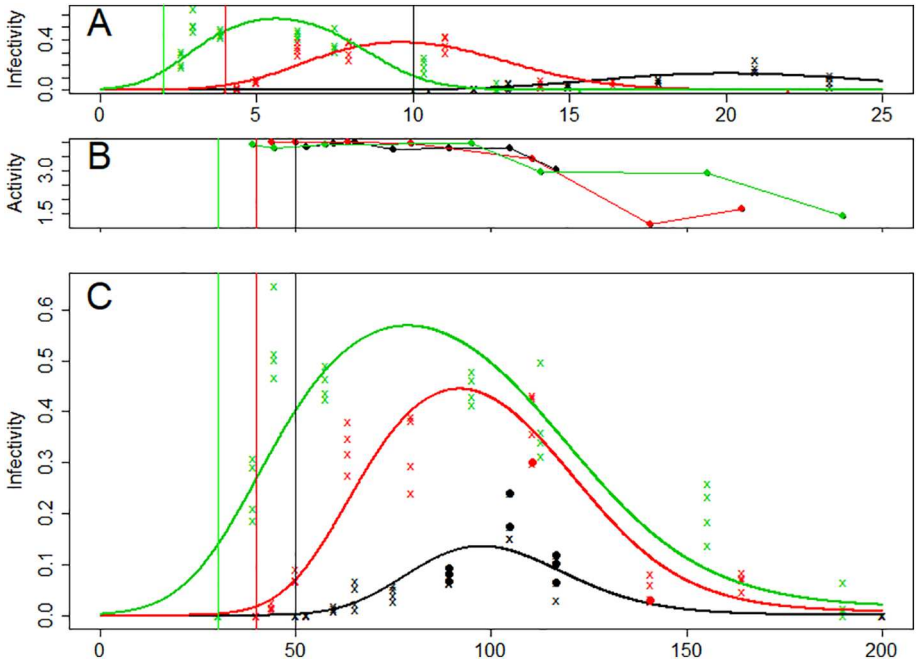

Fig. 1. Copepodid activity and infectivity, at 5 °C (black), 10 °C (red) and 15 °C (green). Vertical lines indicate calculated first appearance of copepodids (Stien et al., 2005). Model results are shown as a solid line. Panel **A**: Infectivity, as a function of age as days post hatch (DPH, indicated on the x axis). Panel **B**: Mean activity score as a function of age as degree-days (DD, indicated at the x-axis in panel C). Panel **C**: Infectivity as a function of DD (indicated on the x axis). Datapoints are denoted with "x" or solid dot "●"; "x" denotes that copepodids were counted on all infected fish. "●" denotes that fish were lost and that copepodid numbers were derived from the remaining infected fish (see materials and methods for further details). (For interpretation of the references to colour in this figure legend, the reader is referred to the web version of this article.)

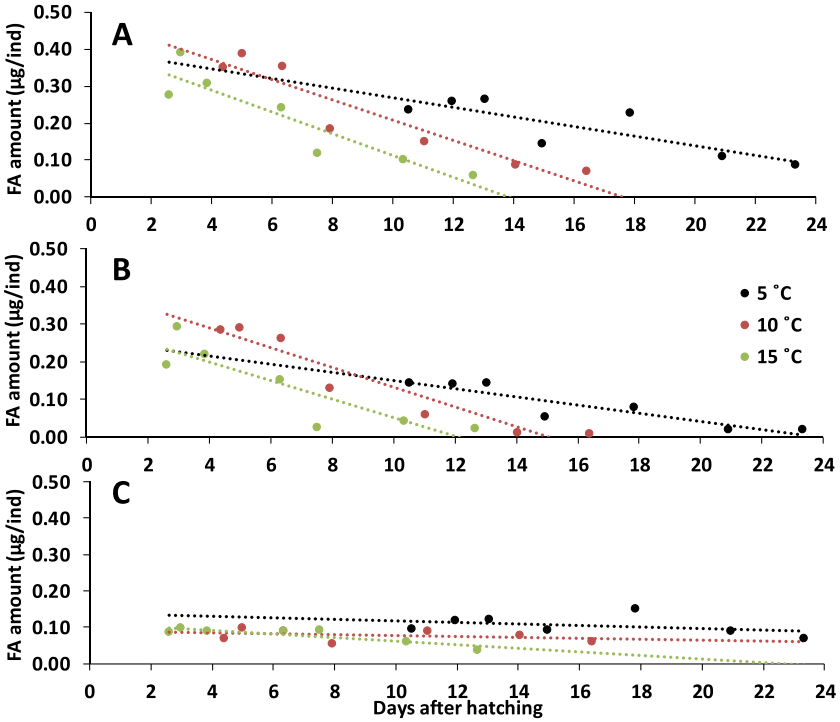

Fig. 2. The amounts of fatty acids (FAs, µg/individual) in the copepodids from the 5 °C (black), 10 °C (red) and 15 °C (green) groups in the total extract (A), the triacylglycerol fraction (B) and the polar lipid fraction (C). (For interpretation of the references to colour in this figure legend, the reader is referred to the web version of this article.)

Table 3
Linear regression of FA amount plotted against days after hatching for total lipid, triacylglycerol (TAG) and polar lipid (PL). Significant *p*-values are in bold.

	Linear regression	R-squared value	P-value
Total lipid			
5 °C	y = −0.013× + 0.399	0.71	**0.018**
10 °C	y = −0.027× + 0.481	0.88	**0.002**
15 °C	y = −0.029× + 0.408	0.84	**0.003**
TAG			
5 °C	y = −0.011× + 0.260	0.84	**0.004**
10 °C	y = −0.026× + 0.393	0.90	**0.001**
15 °C	y = −0.025× + 0.297	0.78	**0.009**
PL			
5 °C	y = −0.002× + 0.139	0.15	0.397
10 °C	y = −0.001× + 0.088	0.11	0.469
15 °C	y = −0.005× + 0.111	0.75	**0.011**

fast reduction of the amount of TAG, while the amount of the polar membrane lipids remained relatively stable over time (Fig. 2A–C). The linear regression equations show that the reduction of TAG was temperature dependent and faster in the 15 °C group than in the 5 °C and 10 °C groups (Fig. 2B, Table 3). At all temperatures, the FA levels were stable for the first 2 days and then started declining thereafter. From the youngest to the oldest copepodids there was a TAG reduction of 87% for the 5 °C group, 97% for the 10 °C group and 89% for the 15 °C group. With the polar lipids, the amount of FAs was relatively stable in the 5 °C and 10 °C groups (only a 28% and 11% reduction, respectively, with the slope of the regressions not being significantly different from zero, Table 3), while in the 15 °C group there was a reduction of 57% (small significant negative slope, Table 3). Remarkably, there were large differences in the lipid amounts in newly molted copepodids between temperature groups. Young copepodids at 5 °C had ≈50% less storage TAG FAs compared with the 10 °C group (Fig. 2A). Interestingly the 5 °C group had slightly higher levels of FAs in the polar fraction (Fig. 2C).

The relative composition of the fatty acid profile of TAG changed over time at all temperatures (Fig. 3A–F). While all fatty acids were depleted over time, PUFA (: polyunsaturated fatty acids) and MUFA (monounsaturated fatty acids) were depleted at a higher rate than SFA, leaving a higher relative content of SFA at the later time points (Fig. 3). This was also supported by principal component analysis where the score plots showed a clustering of the early sampling points (0.5–4 days) separate from the late sampling points (7–13 days), and the loading plot showing that the late samplings points have relatively higher levels of all SFA (from 14:0 to 24:0), while the early samplings points have relatively more MUFA and PUFA (see supplementary data, Fig. S2).

In the polar lipid fraction, the changes in the FA profiles were much less pronounced than for the TAG fraction. The only clear changes in FA profile were a marked decline in PUFA and corresponding increase in SFA seen in the PL fraction at 15 °C (Fig. 3).

3.4. Modelling infection risk in time and space

In the salmon lice dispersal model, we used Eq. (3) to determine the age at which the larvae become infective and Eq. (1) to determine the infectivity after this age. The resulting infectivity profile must be multiplied by a scaling factor of 3.53 to be comparable with the previously used step-function infectivity (Fig. 4). The scaling factor is the ratio of threshold levels (1.8 / 0.51) obtained by the relative operating characteristic (ROC) method (Sandvik et al., 2020) when calibrating the model against lice counts from in-situ observation sentinel cages.

The realistically parameterized ROC analysis revealed that the match between model results and observational data did not change significantly when compared with the infectivity model used previously. The match was slightly improved in low-temperature scenarios and slightly worsened in the higher temperature scenarios. As discussed by Sandvik et al., (2020), the available dataset used to calibrate the model represents a relatively narrow temperature range (8.5 to 13 °C), and minor changes in model fit is therefore to be expected.

The idealized dispersal model experiments with fixed sea water temperature demonstrated that the new infectivity formulation was more sensitive to temperature variations (Fig. 5D–F) than the model presently in use (Fig. 5A–C). In the new formulation, low temperatures give the lice a longer life span (increasing the area of dispersion), but also decreased their infectivity. The old formulation included the first

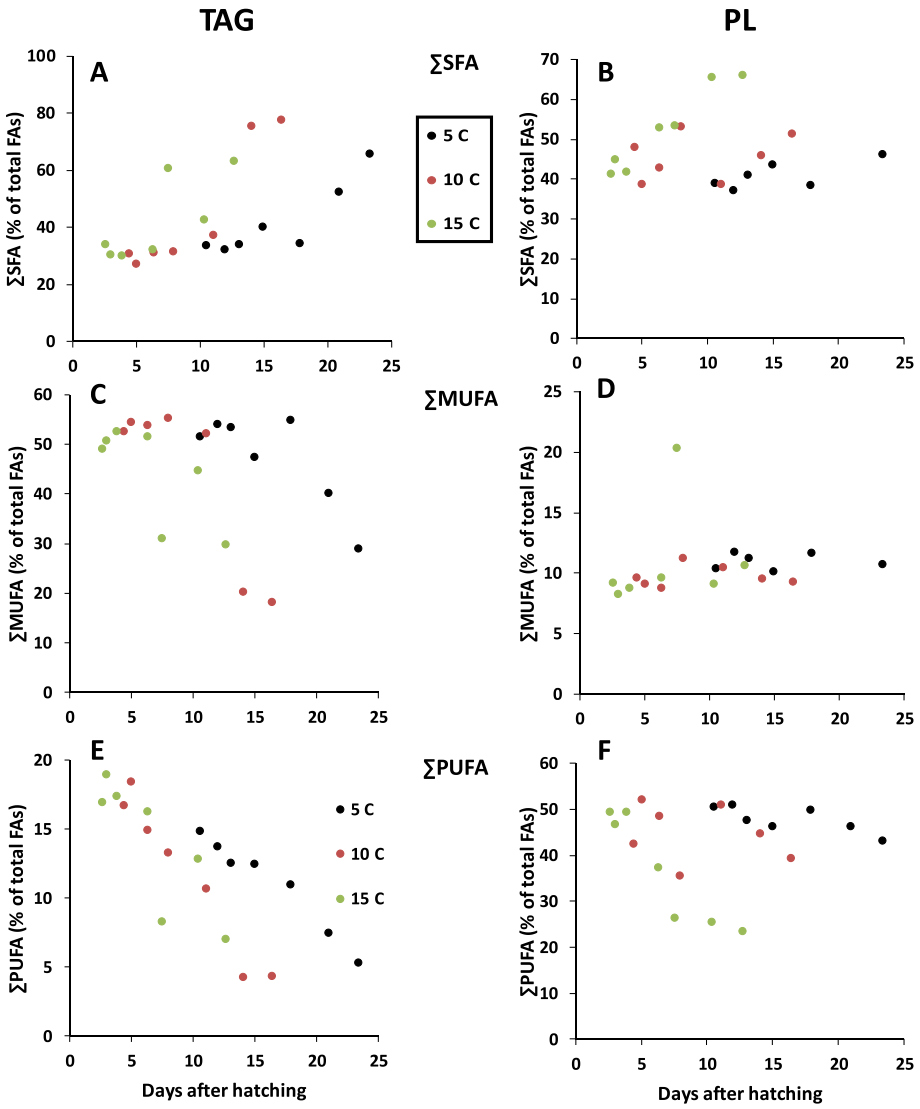

Fig. 3. Changes over time in the relative composition of the fatty acids in the triacylglycerol fraction (A, C, E) and the polar lipid fraction (B, D, F). The plot is showing the sum of saturated fatty acids (ΣSFAs), monounsaturated fatty acids (ΣMUFAs) and polyunsaturated fatty acids (ΣPUFAs) from the 5 °C, 10 °C and 15 °C groups (shown in black, red and green, respectively). Relative data (percentage of total fatty acids) are used to show how the fatty acid (FA) profile changes over time. In absolute terms, all FAs, including SFA decreased over time. The detailed FAs profiles are given as supplementary material, Table S2 and S3. (For interpretation of the references to colour in this figure legend, the reader is referred to the web version of this article.)

effect of increased dispersal range, but not the second effect of declining infectivity. Moreover, lice in the new model have a narrower time window of high infectivity, which gives somewhat less dispersive infectivity patterns over short time periods (hours). This effect is not evident from Fig. 5 as the data are averaged over a longer period.

4. Discussion

Planktonic salmon lice are lecithotrophic and have an infection period limited by depletion of energy stores, and an infectivity that varies with age and temperature (Brooker et al., 2018; Frenzl, 2014; Gravil, 1996; Tucker et al., 2000). However, previous data were

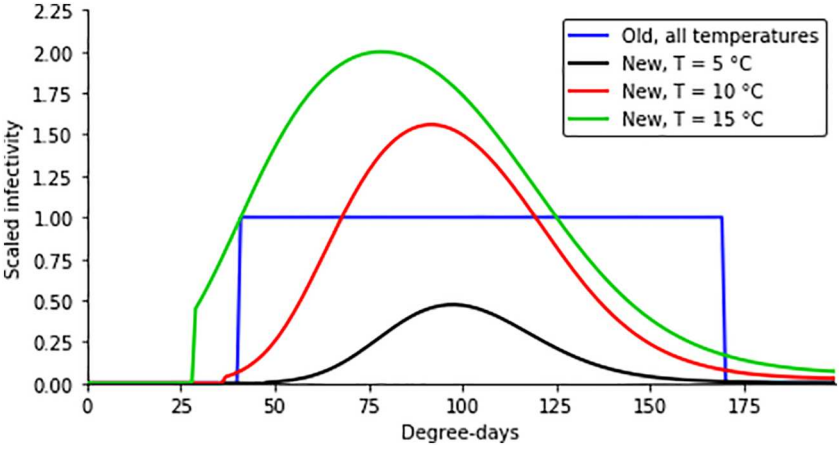

Fig. 4. Scaled infectivity (scaling factor * infectivity) as a function of age in degree-days implemented in the biological-hydrodynamic coupled model. The blue line indicates the constant infectivity profile implemented in current models (e.g. Sandvik et al. (Sandvik et al., 2020) modelled infection risk using this profile is rendered in Fig. 5 A-C). The black, red and green lines indicate the infectivity profiles at 5, 10 and 15 °C from the present study (modelled infection risk results using these are rendered in Fig. 5 D-F). (For interpretation of the references to colour in this figure legend, the reader is referred to the web version of this article.)

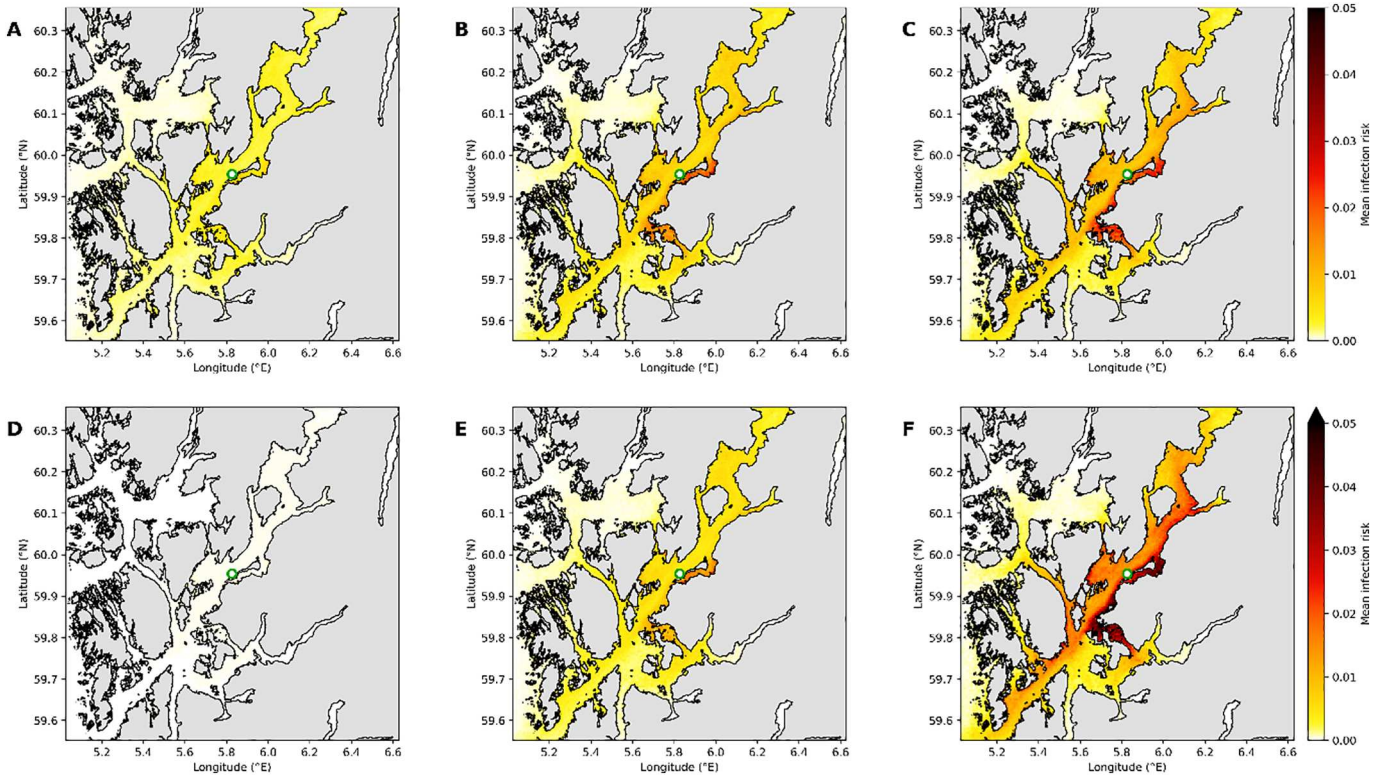

Fig. 5. Modelled infection risk under different temperature scenarios as described in section 2.9. Panels A-C shows the mean infection risk (copepodids m^{-2} * scaled infectivity) in the modelling period (see section 2.9) using a published biological-hydrodynamic coupled model (Sandvik et al., 2020) under the assumption of constant infectivity throughout the copepodid lifespan at 5 °C (A), 10 °C (B) and 15 °C (C). Panels D-F shows the mean infection risk in the modelling period using the infectivity predicted by Eq. (1) at 5 °C (D), 10 °C (E) and 15 °C (F).

insufficient to allow the effect of age and temperature on infectivity to be modelled. Similarly, previous studies on lipid metabolism underlying energy storage depletion have focused on gross energetic patterns, ignoring fine-scale temporal changes and the role of temperature. In the present study we 1) describe the temporal patterns in infectivity at 5, 10 and 15 °C, 2) investigate the explanatory role of copepodid lipid metabolism, and 3) explore the impact of variable infectivity on spatial patterns in salmon louse infection risk.

4.1. Infectivity in ageing cohorts of copepodids at three temperatures

It has earlier been described that copepodid infectivity decreases with senescence and that the newly molted copepodids have limited capability to infect (Frenzl, 2014; Gravil, 1996; Tucker et al., 2000). Only one previous study (Frenzl, 2014) allow tentative identification of the time of peak infectivity; 4 days after molting into copepodids at 14 °C. This equals ≈ 85 DD post hatching, which is close to the 82 DD peak predicted using Eq. (1) at 14 °C. While DD is a useful crude indicator of copepodid maturation and senescence, precise estimation of the time of peak infectivity requires that temperature is considered as a separate model factor, since peak infectivity occurs at a lower DD age at higher temperatures. Whereas maturation and senescence govern the timing of the infectivity peak, the amplitude of the peak appears greater with increasing temperatures until 10–15 °C, remain relatively stable until ~20 °C, and then declines at higher temperatures (Hamre et al., 2019; Samsing et al., 2016). We found both peak and integrated infectivity to increase with warmer temperatures throughout the experimental range (5–15 °C). The peak infectivity was almost 3 times greater at 15 °C compared to 5 °C, providing further support for keeping temperature as a separate model factor. Nevertheless, DD appear to be a useful crude indicator of the timing of copepodid maturation and senescence. Although trends in infectivity are comparable between studies, it is challenging to compare actual infestation levels since 'peak' infestations values from the literature vary enormously. For instance, Frenzl, (2014) reported a peak infectivity of 0.5%, while in Tucker et al., (2000) > 80% of the copepodids successfully attached to a host. These disparities most likely reflect differences in experimental design or conditions, rather than biological variability; while Frenzl, (2014) conducted trials using a flume chamber allowing copepodids to pass the fish only once, Tucker et al., (2000) allowed the copepodids to cohabitate with hosts for 8 h in stagnant aerated water. In the present study, the infection protocol included a 60-min infection period in semi-stagnant water and obtained intermediate peak infection rates relative to the beforementioned studies; 12–56% depending on temperature. Consequently, comparing infection levels between studies with different infection protocols should be done with great caution.

4.2. Lipid composition and metabolism in ageing cohorts of copepodids at three temperatures

The progression of maturation and subsequent senescence is reflected in the linear decrease in total lipid and TAG content in the copepodids over time, which corresponds well with previous findings (Cook et al., 2010; Gravil, 1996; Khan et al., 2018; Tucker et al., 2000). This is a natural result of the copepodids not feeding during the planktonic phase, thus relying on stored energy for development, basic metabolism, and locomotion until a host is located. Lipids constitute the major energy reserve, and it is logical to expect that metabolism and size of the energy reserves will impact on the lifespan, swimming activity and infectivity of the copepodids. Salmon lice kept at 5 °C had far less remaining energy reserves when they molted into copepodids, with 50% of that found in copepodids reared at 10 °C. This may be one contributing factor explaining the reduced infectivity of lice at low temperatures observed here and in earlier studies (Samsing et al.,

2016).

The initial status of our copepodids, with more TAG than PL, and a FA profile dominated by docosahexaenoic acid (DHA, 22:6n-3), 18:1n-9 and 16:0, corresponds well with previous data from salmon lice eggs by Tocher et al., (2010), who also showed that differences in FA profile of eggs and adult lice collected from farmed or wild fish were minor. This likely reflects the importance of salmon blood (in addition to skin and mucus) as food for the adult female lice, as blood has a very conserved FA profile with high DHA content compared to other tissues, regardless of the diet fed to the salmon (Sissener et al., 2016). Hence, data from this study on lice reared in the laboratory on fish fed commercial feed should be considered relevant for lice coming from both farmed and wild salmonid populations.

In addition to the rapid decline in lipid content, distinct changes in the fatty acid profile of TAG were also observed. Preferential mobilization of fatty acids with specific compositions, from lipid stores consisting of a diverse composition of fatty acids, has previously been reported in several food-deprived crustaceans; however, the pattern varies with the species (Koussoroplis et al., 2014; Mezek et al., 2010). Preferential utilization of PUFA over MUFA, and especially SFA, has previously been shown in several copepod species (Koussoroplis et al., 2014). The reason or mechanism behind this is unknown, but hypotheses, such as higher affinity of PUFA substrates to lipases (Raclot, 2003) and optimization of energy storage or buoyancy control, have been suggested (Pond, 2012). There is a natural turnover of cell membrane lipids, acting as a driver for mobilization of FAs from storage (TAG) (Hazel and Williams, 1990). Hence, this could explain why the FAs that are abundant in the polar fraction (such as DHA and other PUFA) decline throughout the study in the TAG fraction.

The structurally important polar lipid FA composition exhibited moderate changes compared to TAGs which have a predominant lipid storage function, as also observed previously in starved copepods (Koussoroplis et al., 2014). This has previously been observed in other food-deprived crustaceans and is likely related to the polar lipids' structural role, and the importance of maintaining the biochemical competency of the cells (Arts and Wainman, 1999; Helland et al., 2003; Sanchez-Paz et al., 2006). Stable levels indicate that the copepodids were able to maintain membrane composition. However, a rapid change in PL composition in the 15 °C group was observed towards the end of the study. Despite a much higher initial PUFA content in the PL compared to TAG, the relative changes in FA profile in these two lipid fractions were somewhat similar in nature, with decreasing PUFA over time, combined with increasing SFA and a modest increase in MUFA. In the freshwater calanoid *Eudiaptomus gracilis*, similar changes in PL FA profile were seen, and the profile remained relatively stable until a sharp decrease in PUFA occurred after day 7 of fasting, coinciding with the near depletion of TAG stores and a mean survival time of 8–9 days at different temperatures (Koussoroplis et al., 2014). Another study demonstrated that a sharp decline in n-3 PUFA cooccurred with high mortality in copepods exposed to food deprivation (Mezek et al., 2010). As PUFA cannot be produced de novo in most animals, including salmon lice, PUFA loss is irreversible unless feeding is resumed. Considering the important roles of PUFAs as structural components of cell membranes, the copepodids reared at 15 °C in our study were likely moribund at the final sampling point, which is also indicated by both their low activity score and low infectivity.

The initial PL composition differed with temperature, with the most notable difference being less SFA in copepods reared at 5 °C. SFA has a high melting point, and hence reduces membrane fluidity, especially at low temperature. This underlines the importance of properly acclimatizing animals before conducting experiments at different temperatures, as a rapid temperature change would not give the animals the time to adjust membrane composition and would probably result in reduced physiological function.

4.3. The effect of temperature and ageing on infection risk

The main effect of including variable infectivity in models is an increased infection risk at higher temperatures. While existing models already predict higher infection risk at warmer temperatures due to increased larval production and accelerated development (Brooker et al., 2018), the addition of the variability in infectivity exacerbates the predicted infection risk at higher temperatures. This finding is in accordance with the general increase in infection levels observed on sea trout during spring and early summer (Grefsrud et al., 2019; Nilsen et al., 2019) and illustrates that the number of copepodids alone does not accurately reflect the infection risk. While the results suggest that the relative geographic infestation risk pattern remains similar, regardless of temperature when simulations are run over a prolonged period, the situation would be different if the scenario were run for periods characterized by diverging current and temperature regimes. It should be noted that the simulations were run with constant temperature in the entire water column over a long period – a highly unrealistic scenario that served to highlight the possible effects of the found infection variability.

Under the realistic setting with variable temperatures in the ROC analysis, the temperature dependent infectivity improved the results at low temperatures while the performance was slightly worsened at the higher ones. In our biological-hydrodynamic coupled model, we have assumed the polynomic infectivity model to be valid across both temperatures and ages. However, the experiments were conducted at constant temperatures, and lice realistically move through micro-environments whereby their temperature history might have a more complex impact on infectivity than the model predicts. Controlled experiments with variable temperatures are needed to further investigate this effect. Validating models is an inherent challenge in model development, and empirical data for model validation may be obtained by, for example, deploying uninfected fish in sentinel cages or by monitoring wild fish and their infection levels (Myksvoll et al., 2018; Sandvik et al., 2016). Unfortunately, the available data obtained using these approaches share a narrow and unmonitored temperature range (sampled during a restricted time window without logging temperature) and hence does not allow for rigorous testing of the modelled temperature effect presented here. However, even though existing observations are insufficient to confirm an improved model performance, we have shown that temperature and age have a large impact on infectivity, and therefore this should be included in biological-hydrodynamic coupled models based on the predicted improvement in performance outside the validated temperature range. Future sentinel cage surveillance efforts should spatiotemporally focus on areas with high infestation pressures and high temperatures.

5. Conclusions

Copepod infectivity is highly influenced by temperature, development and senescence and the use of degree-days as an approximation of biological age is justified albeit imprecise. Copepod infectivity increase with higher temperatures within the experimental range. Copepodid infectivity increased rapidly after molting into copepodids and subsequently declined with senescence, a pattern that should be carefully considered when conducting experiments involving infections with parasitic copepods. Copepod activity decreased with time and hence reflected the observed declining TAG energy stores. Temperature regimes affected not only infectivity, but also the membrane composition as manifested by the differences in phospholipid composition. This illustrates the importance of acclimatizing the experimental animals in experiments involving different or changing temperatures. Model simulations using the derived infectivity profiles indicated that present models simulating salmon louse dispersal and infection risk may underestimate risks at higher temperatures.

Funding

This work was financed by the Norwegian Department of Trade, Industry and Fisheries in its funding to the Institute of Marine Research (internal project no. 14650), and by the Research Council of Norway (project no. 294730).

Authors' Contributions

RSM, SB and SD conceptualized the study. TV, SB, RSM and SD performed the experimental investigation. MSM and RSM performed the formal analyses of the experimental data. NHS and SM performed the lipid investigation and formal analyses of the lipid investigation results. ADS, MDS and PNS performed the biological-hydrodynamic coupled model analyses. RSM, SB, NHS, SM, ADS and PNS wrote the manuscript. RSM finalized the manuscript. All authors revised and approved the final manuscript.

Declaration of Competing Interest

The authors declare that they have no known competing financial, personal, or political interests likely to influence the work reported in this paper.

Acknowledgements

The simulations were performed on resources provided by UNINETT Sigma2 - the National Infrastructure for High Performance Computing and Data Storage in Norway. We thank Martin Biuw and the IMR NALO team for valuable discussions.

Appendix A. Supplementary data

Supplementary data to this article can be found online at https://doi.org/10.1016/j.jembe.2020.151429.

References

Aaen, S.M., Helgesen, K.O., Bakke, M.J., Kaur, K., Horsberg, T.E., 2015. Drug resistance in sea lice: a threat to salmonid aquaculture. Trends Parasitol. 31, 72–81.
Adams, T.P., Aleynik, D., Black, K.D., 2016. Temporal variability in sea lice population connectivity and implications for regional management protocols. Aquacult. Env. Interac. 8, 585–596.
Albretsen, J., Sperrevik, A.K., Staalstrøm, A., Sandvik, A.D., Vikebø, F., Asplin, L., 2011. NorKyst-800 Report No. 1: User Manual and Technical Descriptions. Fisken og Havet. Institute of Marine Research, Bergen, pp. 43.
Aldrin, M., Storvik, B., Kristoffersen, A.B., Jansen, P.A., 2013. Space-time modelling of the spread of Salmon lice between and within Norwegian marine Salmon farms. PLoS One 8.
Anon, 2019. Status for norske laksebestander i 2019. In: Thorstad, E.B., Forseth, T. (Eds.), Rapport fra Vitenskapelig råd for lakseforvaltning Vitenskapelig råd for lakseforvaltning Trondheim, pp. 126.
Arts, M.T., Wainman, B., 1999. Lipids in freshwater zooplankton: selected ecological and physiological aspects. In: Arts, M.T. (Ed.), Lipids in Freshwater Ecosystems. Springer, New York, pp. 71–90.
Asplin, L., Johnsen, I.A., Sandvik, A.D., Albretsen, J., Sundfjord, V., Aure, J., Boxaspen, K.K., 2014. Dispersion of salmon lice in the Hardangerfjord. Mar. Biol. Res. 10, 216–225.
Bjørn, P.A., Finstad, B., Kristoffersen, R., 2001. Salmon lice infection of wild sea trout and Arctic char in marine and freshwaters: the effects of salmon farms. Aquac. Res. 32, 947–962.
Brooker, A.J., Skern-Mauritzen, R., Bron, J.E., 2018. Production, mortality, and infectivity of planktonic larval sea lice, Lepeophtheirus salmonis (Kroyer, 1837): current knowledge and implications for epidemiological modelling. ICES J. Mar. Sci. 75, 1214–1234.
Burridge, L., Weis, J.S., Cabello, F., Pizarro, J., Bostick, K., 2010. Chemical use in salmon aquaculture: a review of current practices and possible environmental effects. Aquaculture 306, 7–23.
Cook, P.F., McBeath, S.J., Bricknell, I.R., Bron, J.E., 2010. Determining the age of individual Lepeophtheirus salmonis (Kr circle divide yer, 1837) copepodids by measuring stored lipid volume; proof of principle. J. Microsc.-Oxford 240, 83–86.
Costello, M.J., 2009. The global economic cost of sea lice to the salmonid farming industry. J. Fish Dis. 32, 115–118.
Dalvin, S., Frost, P., Loeffen, P., Skern-Mauritzen, R., Baban, J., Ronnestad, I., Nilsen, F., 2011. Characterisation of two vitellogenins in the salmon louse Lepeophtheirus salmonis: molecular, functional and evolutional analysis. Dis. Aquat. Org. 94, 211–224.
Finstad, B., Bjørn, P.A., 2011. In: Jones, S., Barnes, R. (Eds.), Present Status and Implications of Salmon Lice on Wild Salmonids in Norwegian Coastal Zones. Wiley-Blackwell, Oxford, pp. 281–305 Salmon lice: an integrated approach to understanding parasite abundance and distribution.
Fjelldal, P.G., Hansen, T.J., Karlsen, O., Wright, D.W., 2019. Effects of laboratory salmon louse infection on Arctic char osmoregulation, growth and survival. Conserv. Physiol. 7, coz072.
Fjørtoft, H.B., Nilsen, F., Besnier, F., Stene, A., Bjorn, P.A., Tveten, A.K., Aspehaug, V.T., Finstad, B., Glover, K.A., 2019. Salmon lice sampled from wild Atlantic salmon and sea trout throughout Norway display high frequencies of the genotype associated with pyrethroid resistance. Aquacult. Env. Interac. 11, 459–468.
Forseth, T., Barlaup, B.T., Finstad, B., Fiske, P., Gjoaester, H., Falkegard, M., Hindar, A., Mo, T.A., Rikardsen, A.H., Thorstad, E.B., Vollestad, L.A., Wennevik, V., 2017. The major threats to Atlantic salmon in Norway. ICES J. Mar. Sci. 74, 1496–1513.
Franceschi, N., Bauer, A., Bollache, L., Rigaud, T., 2008. The effects of parasite age and intensity on variability in acanthocephalan-induced behavioural manipulation. Int. J. Parasitol. 38, 1161–1170.
Frenzl, B., 2014. Understanding Key Factors Associated with the Infection of Farmed Atlantic Salmon by the Salmon Louse, *Lepeophtheirus salmonis*. Institute of Aquaculture. University of Stirling, Stirling, Scotland, UK, pp. 165.
Gonzalez, E.B., de Boer, F., 2017. The development of the Norwegian wrasse fishery and the use of wrasses as cleaner fish in the salmon aquaculture industry. Fish. Sci. 83, 661–670.
Gravil, H.R., 1996. Studies on the biology and ecology of the free swimming larval stages of *Lepeophtheirus salmonis* (Krøyer, 1838) and *Caligus elongatus* Nordmann, 1832 (Copepoda: Caligidae). Institute of Aquaculture. University of Stirling, Stirling, Scotland, UK, pp. 292.
Grefsrud, E.S., Glover, K., Grøsvik, B.E., Husa, V., Karlsen, Ø., Kristiansen, T., Kvamme, B.O., Mortensen, S., Samuelsen, O.B., Stien, L.H., Svåsand, T., 2018. Risikorapport Norsk Fiskeopdrett 2018. Fisken og Havet. Institute of Marine Research, Bergen.
Grefsrud, E.S., Svåsand, T., Glover, K., Husa, V., Hansen, P.K., Samuelsen, O., Sandlund, N., Stien, L.H., 2019. Risikorapport Norsk Fiskeopdrett 2019, Fiske og Havet. Institute of Marine Research, Bergen, Norway, pp. 115.
Grøntvedt, R.N., Nerbøvik, I.K.G., Viljugrein, H., Lillehaug, A., Nilsen, H., Gjevre, A.G., 2015. Thermal de-Licing of Salmonid Fish - Documentation of Fish Welfare and Effect. Norwegian Veterinary Institute's report series. Norwegian Veterinary Institute, Olso, Norway.
Hall, L.M., Murray, A.G., 2018. Describing temporal change in adult female Lepeophtheirus salmonis abundance on Scottish farmed Atlantic salmon at the national and regional levels. Aquaculture 489, 148–153.
Halttunen, E., Gjelland, K.O., Hamel, S., Serra-Llinares, R.M., Nilsen, R., Arechavala-Lopez, P., Skarohamar, J., Johnsen, I.A., Asplin, L., Karlsen, O., Bjorn, P.A., Finstad, B., 2018. Sea trout adapt their migratory behaviour in response to high salmon lice concentrations. J. Fish Dis. 41, 953–967.
Hamre, L.A., Glover, K.A., Nilsen, F., 2009. Establishment and characterisation of salmon louse (Lepeophtheirus salmonis (Kroyer 1837)) laboratory strains. Parasitol. Int. 58, 451–460.
Hamre, L.A., Eichner, C., Caipang, C.M.A., Dalvin, S.T., Bron, J.E., Nilsen, F., Boxshall, G., Skern-Mauritzen, R., 2013. The Salmon louse Lepeophtheirus salmonis (Copepoda: Caligidae) life cycle has only two Chalimus stages. PLoS One 8.
Hamre, L.A., Bui, S., Oppedal, F., Skern-Mauritzen, R., Dalvin, S., 2019. Development of the salmon louse Lepeophtheirus salmonis parasitic stages in temperatures ranging from 3 to 24 degrees C. Aquacult. Env. Interac. 11, 429–443.
Hazel, J.R., Williams, E.E., 1990. The role of alterations in membrane lipid-composition in enabling physiological adaptation of organisms to their physical-environment. Prog. Lipid Res. 29, 167–227.
Helland, S., Nejstgaard, J.C., Fyhn, H.J., Egge, J.K., Bamstedt, U., 2003. Effects of starvation, season, and diet on the free amino acid and protein content of Calanus finmarchicus females. Mar. Biol. 143, 297–306.
Johnsen, I.A., Fiksen, O., Sandvik, A.D., Asplin, L., 2014. Vertical salmon lice behaviour as a response to environmental conditions and its influence on regional dispersion in a fjord system. Aquacult. Env. Interac. 5.
Khan, M.T., Dalvin, S., Nilsen, F., Male, R., 2017. Microsomal triglyceride transfer protein in the ectoparasitic crustacean salmon louse (Lepeophtheirus salmonis). J. Lipid Res. 58, 1613–1623.
Khan, M.T., Dalvin, S., Waheed, Q., Nilsen, F., Male, R., 2018. Molecular characterization of the lipophorin receptor in the crustacean ectoparasite Lepeophtheirus salmonis. PLoS One 13.
Koussoroplis, A.M., Nussbaumer, J., Arts, M.T., Guschina, I.A., Kainz, M.J., 2014. Famine and feast in a common freshwater calanoid: effects of diet and temperature on fatty acid dynamics of Eudiaptomus gracilis. Limnol. Oceanogr. 59, 947–958.
Kristoffersen, A.B., Jimenez, D., Viljugrein, H., Grontvedt, R., Stien, A., Jansen, P.A., 2014. Large scale modelling of salmon lice (Lepeophtheirus salmonis) infection pressure based on lice monitoring data from Norwegian salmonid farms. Epidemics-Neth 9, 31–39.
Lee, R.F., 1975. Lipids of parasitic copepods associated with marine fish. Comp. Biochem. Physiol. B 52, 363–364.
Macnab, V., Barber, I., 2012. Some (worms) like it hot: fish parasites grow faster in warmer water, and alter host thermal preferences. Glob. Chang. Biol. 18, 1540–1548.
Mason, I.B., 1982. A model for assessment of weather forecasts. Aust. Meteorol. Mag. 30, 291–303.
McCallum, H., Fenton, A., Hudson, P.J., Lee, B., Levick, B., Norman, R., Perkins, S.E., Viney, M., Wilson, A.J., Lello, J., 2017. Breaking beta: deconstructing the parasite transmission function. Philos. T R Soc. B 372.

Meier, S., Mjos, S.A., Joensen, H., Grahl-Nielsen, O., 2006. Validation of a one-step extraction/methylation method for determination of fatty acids and cholesterol in marine tissues. J. Chromatogr. A 1104, 291–298.
Mezek, T., Simcic, T., Arts, M.T., Brancelj, A., 2010. Effect of fasting on hypogean (Niphargus stygius) and epigean (Gammarus fossarum) amphipods: a laboratory study. Aquat. Ecol. 44, 397–408.
Mouritsen, K.N., Jensen, K.T., 1997. Parasite transmission between soft-bottom invertebrates: temperature mediated infection rates and mortality in Corophium volutator. Mar. Ecol. Prog. Ser. 151, 123–134.
Myksvoll, M.S., Sandvik, A.D., Albretsen, J., Asplin, L., Johnsen, I.A., Karlsen, O., Kristensen, N.M., Melsom, A., Skardhamar, J., Adlandsvik, B., 2018. Evaluation of a national operational salmon lice monitoring system-from physics to fish. PLoS One 13.
Nilsen, F., Ellingsen, I., Finstad, B., Jansen, P.A., Karlsen, Ø., Kristoffersen, A., Sandvik, A.D., Sægrov, H., Ugedal, O., Vollset, K.W., Myksvoll, M.S., 2017. Vurdering av lakselusindusert villfiskdødelighet per produksjonsområde i 2016 og 2017, Rapport fra ekspertgruppe for vurdering av lusepåvirkning.
Nilsen, R., Serra, R.M.L., Sandvik, A.D., Elvik, K.M.S., Kjær, R., Karlsen, Ø., Finstad, B., 2019. Lakselusinfestasjon på vill laksefisk langs Norskekysten i 2019, Rapport fra Havforskningen. Institue of Marine Research, Bergen, Norway, pp. 97.
Olsen, R.E., Henderson, R.J., 1989. The rapid analysis of neutral and polar marine lipids using double-development Hptlc and scanning densitometry. J. Exp. Mar. Biol. Ecol. 129, 189–197.
Oppedal, F., Samsing, F., Dempster, T., Wright, D.W., Bui, S., Stien, L.H., 2017. Sea lice infestation levels decrease with deeper "snorkel" barriers in Atlantic salmon sea-cages. Pest Manag. Sci. 73, 1935–1943.
Peacock, S.J., Krkosek, M., Bateman, A.W., Lewis, M.A., 2020. Estimation of spatio-temporal transmission dynamics and analysis of management scenarios for sea lice of farmed and wild salmon. Can. J. Fish. Aquat. Sci. 77, 55–68.
Pike, A.W., Wadsworth, S.L., 1999. Sealice on salmonids: their biology and control. Adv. Parasitol. 44, 233–337.
Pond, D.W., 2012. The physical properties of lipids and their role in controlling the distribution of zooplankton in the oceans. J. Plankton Res. 34, 443–453.
Raclot, T., 2003. Selective mobilization of fatty acids from adipose tissue triacylglycerols. Prog. Lipid Res. 42, 257–288.
Salama, N.K.G., Collins, C.M., Fraser, J.G., Dunn, J., Pert, C.C., Murray, A.G., Rabe, B., 2013. Development and assessment of a biophysical dispersal model for sea lice. J. Fish Dis. 36, 323–337.
Samsing, F., Oppedal, F., Dalvin, S., Johnsen, I., Vagseth, T., Dempster, T., 2016. Salmon lice (Lepeophtheirus salmonis) development times, body size, and reproductive outputs follow universal models of temperature dependence. Can. J. Fish. Aquat. Sci. 73, 1841–1851.
Sanchez-Paz, A., Garcia-Carreno, F., Muhlia-Almazan, A., Peregrino-Uriarte, A.B., Hernandez-Lopez, J., Yepiz-Plascencia, G., 2006. Usage of energy reserves in crustaceans during starvation: status and future directions. Insect. Biochem. Molec. 36, 241–249.
Sandvik, A.D., Bjorn, P.A., Adlandsvik, B., Asplin, L., Skardhamar, J., Johnsen, I.A., Myksvoll, M., Skogen, M.D., 2016. Toward a model-based prediction system for salmon lice infestation pressure. Aquacult. Env. Interac. 8, 527–542.
Sandvik, A.D., Johnsen, I.A., Myksvoll, M.S., Sævik, P.N., Skogen, M.D., 2020. Prediction of the salmon lice infestation pressure in a Norwegian fjord. ICES J. Mar. Sci. 77, 746–756.
Sissener, N.H., Torstensen, B.E., Stubhaug, I., Rosenlund, G., 2016. Long-term feeding of Atlantic salmon in seawater with low dietary long-chain n-3 fatty acids affects tissue status of the brain, retina and erythrocytes. Brit. J. Nutr. 115, 1919–1929.
Skardhamar, J., Albretsen, J., Sandvik, A.D., Lien, V.S., Myksvoll, M.S., Johnsen, I.A., Asplin, L., Adlandsvik, B., Halttunen, E., Bjorn, P.A., 2018. Modelled salmon lice dispersion and infestation patterns in a sub-arctic fjord. ICES J. Mar. Sci. 75, 1733–1747.
Skern-Mauritzen, R., Torrissen, O., Glover, K.A., 2014. Pacific and Atlantic Lepeophtheirus salmonis (Kroyer, 1838) are allopatric subspecies: Lepeophtheirus salmonis salmonis and L. salmonis oncorhynchi subspecies novo. BMC Genet. 15.
Stien, A., Bjorn, P.A., Heuch, P.A., Elston, D.A., 2005. Population dynamics of salmon lice Lepeophtheirus salmonis on Atlantic salmon and sea trout. Mar. Ecol. Prog. Ser. 290, 263–275.
Stien, L.H., Lind, M.B., Oppedal, F., Wright, D.W., Seternes, T., 2018. Skirts on salmon production cages reduced salmon lice infestations without affecting fish welfare. Aquaculture 490, 281–287.
Taranger, G.L., Karlsen, O., Bannister, R.J., Glover, K.A., Husa, V., Karlsbakk, E., Kvamme, B.O., Boxaspen, K.K., Bjorn, P.A., Finstad, B., Madhun, A.S., Morton, H.C., Svasand, T., 2015. Risk assessment of the environmental impact of Norwegian Atlantic salmon farming. ICES J. Mar. Sci. 72, 997–1021.
Thompson, C.R.S., Fields, D.M., Bjelland, R.M., Chan, V.B.S., Durif, C.M.F., Mount, A., Runge, J.A., Shema, S.D., Skiftesvik, A.B., Browman, H.I., 2019. The planktonic stages of the salmon louse (Lepeophtheirus salmonis) are tolerant of end-of-century pCO(2) concentrations. Peerj 7.
Tocher, J.A., Dick, J.R., Bron, J.E., Shinn, A.P., Tocher, D.R., 2010. Lipid and fatty acid composition of parasitic caligid copepods belonging to the genus Lepeophtheirus. Comp. Biochem. Physiol. B 156, 107–114.
Torrissen, O., Jones, S., Asche, F., Guttormsen, A., Skilbrei, O.T., Nilsen, F., Horsberg, T.E., Jackson, D., 2013. Salmon lice - impact on wild salmonids and salmon aquaculture. J. Fish Dis. 36, 171–194.
Tucker, C.S., Sommerville, C., Wootten, R., 2000. An investigation into the larval energetics and settlement of the sea louse, Lepeophtheirus salmonis, an ectoparasitic copepod of Atlantic salmon, Salmo salar. Fish. Pathol. 35, 137–143.
Vollset, K., Nilsen, F., Ellingsen, I., Finstad, B., Helgesen, K., Karlsen, Ø., Sandvik, A., Sægrov, H., Ugedal, O., Qviller, L.O., Dalvin, S., 2019. Vurdering av lakselusindusert villfiskdødelighet per produksjonsområde i 2019 (in Norwegian). Rapport fra ekspertgruppe for vurdering av lusepåvirkning, Bergen. pp. 84.
Wasta, Z., Mjos, S.A., 2013. A database of chromatographic properties and mass spectra of fatty acid methyl esters from omega-3 products. J. Chromatogr. A 1299, 94–102.